Time-resolved radiation chemistry: Dynamics of electron attachment to uracil following UV excitation of iodide-uracil complexes

Sarah B. King, Margaret A. Yandell, Anne B. Stephansen, and Daniel M. Neumark

Citation: The Journal of Chemical Physics **141**, 224310 (2014); doi: 10.1063/1.4903197
View online: http://dx.doi.org/10.1063/1.4903197
View Table of Contents: http://scitation.aip.org/content/aip/journal/jcp/141/22?ver=pdfcov
Published by the AIP Publishing

Time-resolved radiation chemistry: Dynamics of electron attachment to uracil following UV excitation of iodide-uracil complexes

Sarah B. King,[1] Margaret A. Yandell,[1] Anne B. Stephansen,[2] and Daniel M. Neumark[1,3,a)]
[1]*Department of Chemistry, University of California, Berkeley, California 94720, USA*
[2]*Department of Chemistry, University of Copenhagen, Universitetsparken 5, DK-2100 København Ø, Denmark*
[3]*Chemical Sciences Division, Lawrence Berkeley National Laboratory, Berkeley, California 94720, USA*

(Received 26 September 2014; accepted 19 November 2014; published online 11 December 2014)

Electron attachment to uracil was investigated by applying time-resolved photoelectron imaging to iodide-uracil (I^-U) complexes. In these studies, an ultraviolet pump pulse initiated charge transfer from the iodide to the uracil, and the resulting dynamics of the uracil temporary negative ion were probed. Five different excitation energies were used, 4.00 eV, 4.07 eV, 4.14 eV, 4.21 eV, and 4.66 eV. At the four lowest excitation energies, which lie near the vertical detachment energy of the I^-U complex (4.11 eV), signatures of both the dipole bound (DB) as well as the valence bound (VB) anion of uracil were observed. In contrast, only the VB anion was observed at 4.66 eV, in agreement with previous experiments in this higher energy range. The early-time dynamics of both states were highly excitation energy dependent. The rise time of the DB anion signal was ∼250 fs at 4.00 eV and 4.07 eV, ∼120 fs at 4.14 eV and cross-correlation limited at 4.21 eV. The VB anion rise time also changed with excitation energy, ranging from 200 to 300 fs for excitation energies 4.00–4.21 eV, to a cross-correlation limited time at 4.66 eV. The results suggest that the DB state acts as a "doorway" state to the VB anion at 4.00–4.21 eV, while direct attachment to the VB anion occurs at 4.66 eV.
 [http://dx.doi.org/10.1063/1.4903197]

I. INTRODUCTION

In recent years, numerous experiments have implicated low energy electrons in both single- and double-strand breaks of DNA.[1,2] Theory predicts that this damage occurs via cleavage of the sugar phosphate backbone following electron transfer from the nucleobase, the original electron acceptor.[3–5] Thymine and its RNA analog, uracil, have been investigated both experimentally and theoretically to understand how low-energy electrons interact with nucleobases.[6–11] While dissociative electron attachment (DEA) experiments show that electrons as low as 0.6–1.0 eV can cause fragmentation of the nitrogen-hydrogen bonds in uracil,[12–14] the precise mechanism by which the low energy electrons interact with these nucleobases is not fully understood. In this work, we explore early-time electron attachment dynamics to the RNA base uracil via time-resolved photoelectron (PE) imaging of the iodide-uracil (I^-U) complex at a variety of excitation energies both near and well above the vertical detachment energy (VDE) of I^-U, expanding on earlier studies[15,16] performed only at excitation energies well above the VDE.

Uracil in the gas phase binds an excess electron in a dipole bound (DB) ground state, with a conventional valence bound (VB) state of the anion calculated to be slightly higher in energy.[17,18] In the DB state, the excess electron is bound in a diffuse orbital by the field of the molecular dipole moment, largely outside the molecular core;[19] such states can be supported by molecules with dipole moments greater than 2 Debye.[20] The VB state of uracil binds the excess electron in a conventional π^* molecular orbital.[21] In DEA experiments, coupling between the DB and VB states of the uracil anion has been invoked to interpret the low energy (0.6–1 eV) DEA resonances, with the DB anion assumed to act as a "doorway" state.[13] Calculations predict that a DB to VB anion transition occurs via a puckering of the uracil ring and out of plane motion of the C6 hydrogen (atomic numbering shown in Figure 1),[22,23] with an energy barrier ranging from 36 to 178 meV, depending on the calculation method.[22,24,25]

DB and VB states of anions can be distinguished in PE spectroscopy by differences in peak width and electron binding energy.[26,27] DB electrons minimally perturb the neutral molecular geometry and DB anions are characterized in their PE spectrum by a very narrow peak and a vertical detachment energy (VDE), defined as the difference in energy between the neutral and the anion at the geometry of the anion, that is generally less than 0.1 eV.[5] Since the geometries of the DB anion and neutral are very similar, the VDE of the DB state is approximately the same as the adiabatic electron affinity (AEA) of the neutral, where the AEA is defined as the energy difference between the electronic and vibrational ground states of the anion and neutral.

In contrast, VB anions often have a different geometry than the neutral, resulting in a much wider peak in their PE spectrum. The PE spectrum of bare uracil anions in the gas phase show evidence only for the DB anion, with a VDE of 93 ± 3 meV.[18] PE spectra for uracil complexed with a sufficiently polarizable species (i.e., xenon) have peaks due to both the DB and VB anions.[26] Only the VB anion is present when uracil is complexed with a single H_2O molecule[26] and

a)Author to whom correspondence should be addressed. Electronic mail: dneumark@berkeley.edu

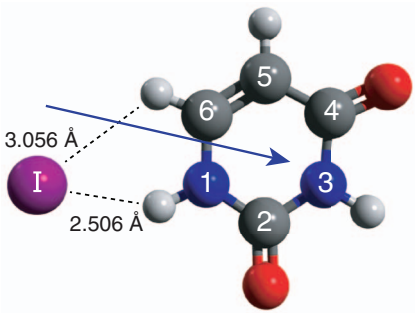

FIG. 1. Calculated structure of the iodide-uracil cluster.[16] The blue arrow indicates the direction of the calculated dipole moment of the neutral uracil molecule.

continued water solvation shifts the VB anion to higher binding energies.[28] A photoelectron spectrum of the bare uracil VB anion has not been measured but theory predicts a VDE of 600 meV[29] and an AEA between −50 meV and 40 meV.[5,29–33] Experimental extrapolation from PE spectra of $U^-(H_2O)_n$ clusters yields an estimate of 150 ± 120 meV for the adiabatic electron binding energy of the VB anion.[28]

Iodide-uracil (and iodide-thymine) complexes have been previously studied in our laboratory using one-photon and time-resolved PE spectroscopy.[15,16] Single photon PE spectra of I⁻U identified the ground state complex as a negative iodide atom complexed to a neutral uracil molecule with a VDE of 4.11 eV;[16] the calculated ground state geometry of I⁻U from that work is shown in Figure 1. Absorption spectra of the I⁻U complex and U⁻ photofragment action spectra have not been recorded.

In the time-resolved PE spectroscopy experiments,[34] a UV excitation pulse ($h\nu_1$) induced electron transfer from the iodide to the uracil molecule, and the resulting transient negative ion was photodetached by a near IR pulse ($h\nu_2$) after a known time delay, according to Eq. (1),

$$I^- \cdot U \xrightarrow{h\nu_1} I \cdots U^- \xrightarrow{\Delta t, h\nu_2} I \cdots U + e^-(eKE = h\nu_2 - eBE). \quad (1)$$

UV excitation energies from 4.69 to 4.90 eV were used, significantly above the VDE of I⁻U, and those experiments were considered analogous to electron scattering experiments. The excitation energies 4.69–4.90 eV corresponded to collision energies, $E_c = h\nu - VDE(I^-U)$, of 580–790 meV. Coupling between DB anions and σ^* anions of uracil has been invoked to explain resonances in DEA spectra at >0.6 eV electron kinetic energy,[13] within the range of the collision energies studied in the time-resolved PE experiments. However, only the VB anion of uracil was observed as a transient species, with no evidence of a DB anion of uracil. The VB anion appeared on a cross-correlation limited time scale (<150 fs) and decayed bi-exponentially with time constants of 400–700 fs and 12–52 ps, depending on excitation energy. These time constants were attributed to autodetachment of the temporary negative ion I · · · U⁻, both before and after loss of the iodine atom.

To gain further insight into the role of DB and VB states in these experiments, we carried out time-resolved PE studies on two model systems, iodide-acetonitrile and iodide-nitromethane.[35] The acetonitrile anion is a DB state, with no low-lying VB state.[36,37] Nitromethane, however, supports both low-lying DB and VB anions with a VB anionic ground state.[27] UV-initiated charge transfer from the iodide to the acetonitrile or nitromethane molecule was investigated using excitation energies near the VDE of the binary complex. Experiments on I^-CH_3CN complexes showed evidence only for the DB anion of acetonitrile, while experiments on $I^-CH_3NO_2$ clusters showed initial formation of the DB CH_3NO_2 anion decaying to the VB anion on a timescale of 400–600 fs.[35]

The work on I^-CH_3CN and $I^-CH_3NO_2$ suggested that the early-time electron attachment dynamics in I⁻U might be substantially different at excitation energies closer to the VDE of the complex. In this paper, we carry out such experiments, using excitation energies ranging from 4.00 to 4.21 eV, below and above the VDE of I⁻U, as well as at 4.66 eV, in the range of our previous experiments. We find that the early-time attachment dynamics are highly sensitive to excitation energy and observe formation of both the DB and VB anions of uracil at all excitation energies near the VDE. Below the VDE, both DB and VB anions appear with 200–300 fs rise times. Above the VDE, the DB anion appears with a less prominent ∼120 fs rise time and within the cross-correlation for 4.14 and 4.21 eV, respectively, while the VB anion has the same 200–300 fs rise time from 4.00 to 4.21 eV. In contrast, at 4.66 eV, no DB state is seen, and the VB state appears within our cross-correlation. Evidence suggests that the DB state acts as a doorway to the VB state near the VDE, but that electrons attach directly to the VB state at 4.66 eV, a result with possible implications for interpreting the DEA experiments.

II. EXPERIMENTAL

The time-resolved PE spectrometer used in these experiments has been described in detail in Ref. 38 and 39. I⁻U clusters were formed by flowing 50 psig neon over a reservoir containing iodomethane through an Even-Lavie pulsed solenoid valve containing uracil heated to 205 °C. The resulting gas mixture was expanded into vacuum through a ring-filament ionizer attached to the valve body. The femtosecond laser system is a KM Labs Griffin oscillator and a Dragon amplifier that outputs pulses centered at 790 nm with a 1 kHz repetition rate. The excitation pulses used in these experiments were generated by frequency-doubling the output of a Light Conversion TOPAS-C optical parametric amplifier (OPA), resulting in laser pulses that were tuned from 4.00 eV to 4.66 eV with approximately 5–10 μJ/pulse at the interaction region, depending on the efficiency of the OPA. The laser fundamental served as the probe pulse in these experiments with approximately 80 μJ/pulse. The cross-correlation of the pump and probe pulses was less than 150 fs. The photoelectrons resulting from the pump-probe experiment were energy-analyzed by velocity map imaging (VMI) onto a position sensitive detector.[40] These VMI images were then processed using the BASEX reconstruction method.[41]

III. RESULTS AND ANALYSIS

Experiments were conducted at five excitation energies: 4.00 eV, 4.07 eV, 4.14 eV, 4.21 eV, and 4.66 eV. For the

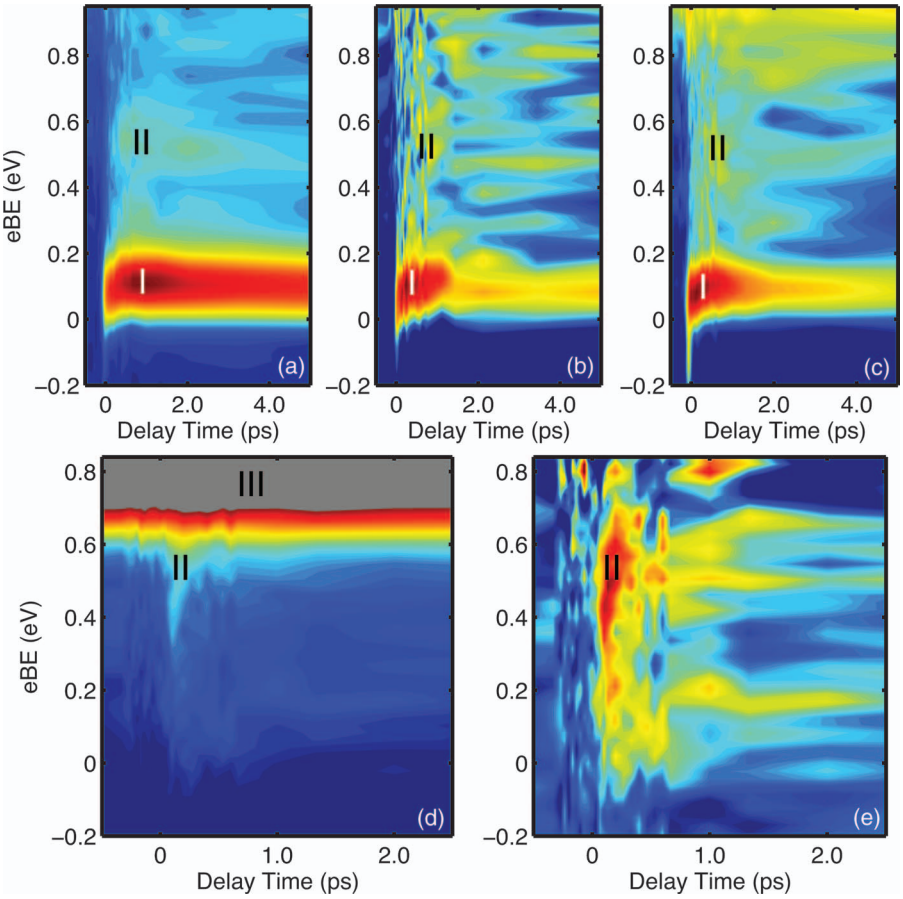

FIG. 2. Time-resolved photoelectron spectra of iodide-uracil at excitation energies (a) 4.07 eV (−40 meV), (b) 4.14 eV (30 meV), (c) 4.21 eV (100 meV) and 4.66 eV (550 meV) both raw (d) and negative time background subtracted (e), all probed with 1.58 eV.

remainder of the paper, these excitation energies will be referenced relative to VDE(I^-U) = 4.11 eV, as −110 meV, −40 meV, 30 meV, 100 meV, and 550 meV. Figure 2 shows time-resolved PE spectra obtained at −40 meV (Fig. 2(a)), 30 meV (Fig. 2(b)), 110 meV (Fig. 2(c)), and 550 meV (Figs. 2(d) and 2(e)). Figure 2(d) is a raw time-resolved spectrum and Fig. 2(e) is background subtracted. The y-axis is electron binding energy (eBE), defined as eBE = $h\nu_{probe}$ − eKE, where $h\nu_{probe}$ = 1.58 eV, the photon energy of the probe pulse.

The spectra comprise three distinct features labeled I–III. Features I and II are transient features due to probe detachment from the photo-excited complex, while feature III is primarily due to direct detachment of the ground state iodide-uracil cluster induced by the excitation pulse.[15,16,35] Feature III is very high in intensity compared to features I and II, and in Figure 2(d) it is largely off scale and colored grey. Upon negative-time background subtraction, feature III is only seen as residual noise in Figure 2(e). It should be noted that at 30 meV and 100 meV, there is some electron signal near $\Delta t = 0$ between −0.2 eV and 0 eV eBE, in the vicinity of feature I. This electron signal is attributed to two-color two-photon detachment of the iodide-uracil complex, observed previously with I^- nitromethane and I^- acetonitrile,[35] and is not included in the analysis of feature I.

Feature I is a narrow feature appearing at low eBE, between 0 and 0.2 eV, and observed at excitation energies −110 meV to 100 meV. The peak of feature I evolves slightly with pump-probe delay time, approaching 95 ± 5 meV at long times. Feature II is a broad, low intensity feature spanning the energy range from 0.3 to 0.7–0.8 eV and is observed at all excitation energies studied. Based on previous experiments, features I and II can be identified as photo-detachment from the dipole bound (DB) and valence bound (VB) anions of uracil, respectively.[16,35]

Table I reports the intensity ratio of feature I to feature II, which was measured at a set time delay where both features are close to their maxima, approximately 400–500 fs. This ratio decreases with increasing excitation energy. The 550 meV data are in agreement with previously published results where the iodide-uracil clusters were formed by expansion in argon instead of neon.[16]

In order to quantify the peak shifting of feature I, the photoelectron spectrum of the feature can be fit with a Gaussian function at all pump-probe delays with non-zero intensity. The peak in the eBE is the VDE of the feature and Figure 3 shows the evolution of the VDE of feature I versus pump-probe delay at −40 meV. The peak shifting shown is representative of that observed at all other excitation energies where feature I is present. At zero pump-probe delay, the VDE of feature I is approximately 75 meV and rises to approximately 115 meV by 700 fs before decaying back to a longtime value of 95 ± 5 meV. This asymptotic value lies within error bars of the previously measured value of the VDE

TABLE I. Lifetimes and decay coefficient ratios for features I and II, where τ_1 is the rise time (if applicable) and τ_2 and τ_3 are decay times. The energies in parentheses refer to the energy definition given in the beginning of Section III, where the excitation energies are defined relative to the VDE(I⁻U) = 4.11 eV.

Excitation energy	τ_1	τ_2	τ_3	$A_1/(A_2+A_3)$	Ratio of I/II
			Feature I		
4.00 eV (−110 meV)	240 ± 30 fs	8.5 ± 1.2 ps	2000 ± 600 ps	−0.44	1.90
4.07 eV (−40 meV)	260 ± 50 fs	7.1 ± 0.7 ps	1200 ± 100 ps	−0.46	1.41
4.14 eV (30 meV)	120 ± 90 fs	5.0 ± 0.6 ps	500 ± 130 ps	−0.28	1.04
4.21 eV (100 meV)	...	1.7 ± 0.4 ps	30 ± 10 ps	...	0.83
			Feature II		
4.00 eV (−110 meV)	264 ± 15 fs	16 ± 2 ps	460 ± 80 ps	−0.77	
4.07 eV (−40 meV)	200 ± 20 fs	13.9 ± 1.4 ps	450 ± 40 ps	−0.76	
4.14 eV (30 meV)	220 ± 40 fs	5.6 ± 1.5 ps	80 ± 30 ps	−0.74	
4.21 eV (100 meV)	300 ± 150 fs	5.0 ± 2.0 ps	80 ± 40 ps	−0.48	
4.66 eV (550 meV)	...	0.41 ± 0.04 ps	35 ± 13 ps	...	

of the bare uracil DB anion.[18] Feature II does not display any notable peak shifting and is too diffuse to be fit to an analytical function.

Features I and II both undergo intensity changes with varying pump-probe delay. Since the intensity of feature I changes in both time and energy space, the feature is integrated by a set amount around the peak at each pump-probe delay to minimize the effect of energy shifting on the intensity changes. Feature II is integrated over a fixed eBE range for every pump-probe delay. The intensities of both features for all short delays are shown in Figure 4. At −40 meV, feature I has a measurably slower rise time than the cross-correlation (Figure 4(a)), while at 100 meV, feature I rises on a cross-correlation limited time before decaying (Figure 4(c)). Between these two excitation energies, at 30 meV, feature I has a distinct rise time although faster and less prominent than at −40 meV. At longer times, as shown in Figure 5, feature I decays bi-exponentially, with considerably faster decay at 110 meV than at −40 meV.

Feature II exhibits two different early-time dynamic regimes. At lower excitation energies −110 meV to 100 meV, feature II exhibits a clear non-zero rise time, and it rises more slowly than feature I in all three panels (Figures 4(a)–4(c)). However, at 550 meV the VB anion rises on a cross-correlation limited time scale before decaying (Figure 4(d)). For all excitation energies studied, feature II eventually decays bi-exponentially (Figures 5(a)–5(c)).

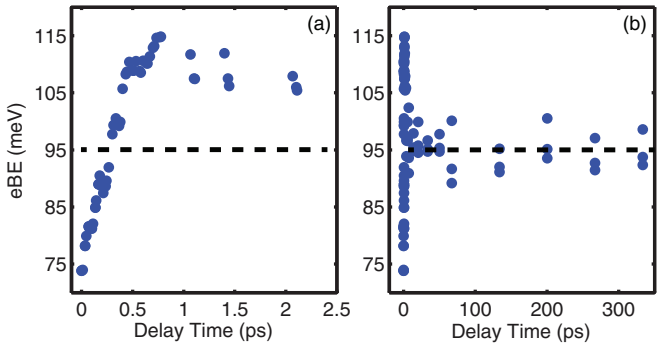

FIG. 3. Time evolution of the vertical detachment energy of feature I at 4.07 eV (−40 meV) shown at both (a) short times and (b) long times. The dashed line indicates the longtime VDE of 95 ± 5 meV.

The normalized intensity evolution of both features can be fit to a sum of exponential functions convoluted with an experimental response function, Eq. (2),

$$I(t) = \frac{1}{\sigma_{CC}\sqrt{2\pi}} \exp\left(\frac{-t^2}{2\sigma_{CC}^2}\right) * \begin{cases} I_0, t < 0 \\ I_0 + \sum_i A_i \exp\left(\frac{-t}{\tau_i}\right), t \geq 0 \end{cases}. \quad (2)$$

Feature I is fit well with three coefficients and time-constants at −110 meV, −40 meV, and 30 meV comprising a mono-exponential rise and bi-exponential decay. At 100 meV, feature I is fit well with only two coefficients and time-constants, capturing the cross-correlation limited rise and bi-exponential decay of the feature. Feature II is fit well with three

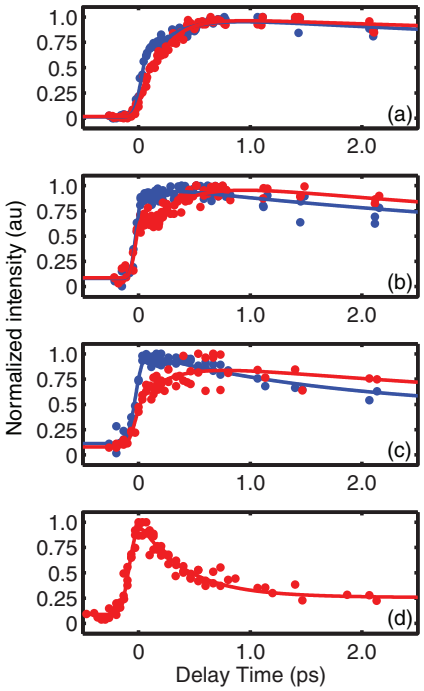

FIG. 4. Normalized integrated intensities for features I and II, where feature I is in blue and feature II is in red at (a) 4.07 eV (−40 meV), (b) 4.14 eV (30 meV), (c) 4.21 eV (100 meV), and (d) 4.66 eV (550 meV).

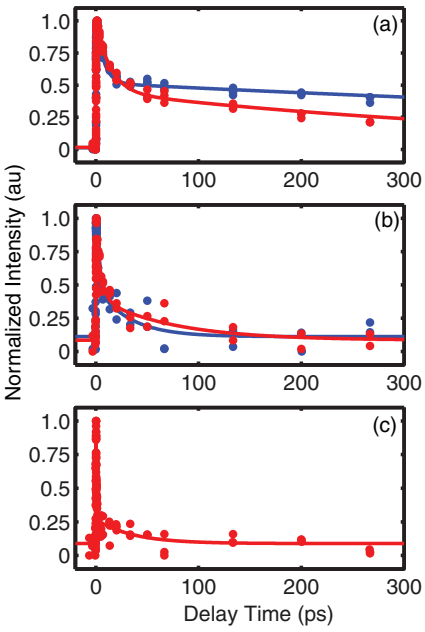

FIG. 5. Normalized Intensities for features I and II at long time, feature I is shown in blue, feature II is shown in red at excitation energies (a) 4.07 eV (−40 meV), (b) 4.21 eV (100 meV), and (c) 4.66 eV (550 meV).

coefficients and time-constants at −110 meV to 100 meV, a mono-exponential rise and bi-exponential decay. However at 550 meV, feature II is fit well with two coefficients and time-constants, capturing the cross-correlation limited rise and bi-exponential decay at that excitation energy. Where applicable, A_1 and τ_1 capture any mono-exponential rise and A_2, A_3, τ_2, and τ_3 capture the bi-exponential decay. Data collected at the same excitation energy were fit concatenately. Table I shows all lifetimes τ_i and the ratio of the rising component to the decay components, $A_1/(A_2 + A_3)$, at the five different excitation energies. Note that when $A_1 = 0$, the rise time is cross-correlation limited.

Features I and II exhibit long time bi-exponential decay regardless of early-time behavior. As seen in previous papers from our group,[15,16,42] this kind of bi-exponential decay can be explained with a kinetic model like Scheme 1.

The bi-exponential decay lifetimes in Table I can be related to the time constants of the kinetic model by (3),

$$\tau_2 = \frac{1}{k_1 + k_2} \quad \tau_3 = \frac{1}{k_3}. \tag{3}$$

According to Knee *et al.*,[43] by using the fraction of the fast decay to the total decay signal, $F_{A_2} = A_2/(A_2 + A_3)$, rate constants can be extracted from the bi-exponential lifetimes according to (4).

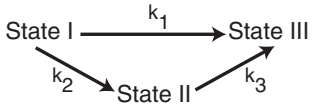

SCHEME 1. Describing bi-exponential decay kinetics.

$$\begin{aligned} k_1 &= F_{A_2}\left(\frac{1}{\tau_2} - \frac{1}{\tau_3}\right) + \frac{1}{\tau_3}, \\ k_2 &= \frac{1}{\tau_2} - k_1, \\ k_3 &= \frac{1}{\tau_3}. \end{aligned} \tag{4}$$

Fractions and rate constants are summarized in Table II. The nature of States I–III is considered in more detail in Sec. IV D.

IV. DISCUSSION

The dynamics of iodide-uracil clusters following UV initiated charge transfer are highly sensitive to excitation energy. As the excitation energy is increased, the following trends are observed: (i) shifting of the DB anion VDE is the same at all excitation energies, (ii) starting at −40 meV, the DB anion rise time τ_1 and the ratio $|A_1|/(A_2 + A_3)$ decrease, and by 100 meV the DB anion appears within the cross-correlation without any observed rise time, (iii) the VB anion rise time is approximately the same from −110 meV to 100 meV but is cross-correlation limited at 550 meV, (iv) the ratio of the DB anion to the VB anion decreases with the DB anion disappearing completely by 550 meV, and (v) the bi-exponential decay lifetimes decrease for both the DB and VB anion. In this section, we consider the underlying electron attachment and detachment dynamics responsible for these trends.

A. Early-time dynamics of the uracil dipole bound anion

At early times, the VDE of the DB anion shifts with pump-probe delay, as shown in Figure 3. Shifts of this magnitude have been seen in the early-time dynamics of other iodide-solvent complexes.[35,44–46] Comparison to theory suggests that these shifts result from two effects: the excited state interaction of the neutral iodine atom with the diffuse electron associated with the nascent negative ion formed by photoexcitation,[47] and, in the case of multiple solvating

TABLE II. Rate constants and fractions for bi-exponential decay kinetics.

Excitation energy	Feature I				Feature II			
	$k_1(10^{10}\ s^{-1})$	$k_2(10^{10}\ s^{-1})$	$k_3(10^{10}\ s^{-1})$	F_{A2}	$k_1(10^{10}\ s^{-1})$	$k_2\ (10^{10}\ s^{-1})$	$k_3\ (10^{10}\ s^{-1})$	F_{A2}
4.00 eV	6.0	5.6	0.05	0.52	3.5	2.6	0.22	0.55
4.07 eV	7.1	6.9	0.08	0.50	4.1	3.0	0.22	0.56
4.14 eV	15	5.8	0.20	0.71	11	6.4	1.2	0.61
4.21 eV	35	23	3.2	0.58	13	7.3	1.3	0.63
4.66 eV	...	...	...	...	200	41	2.8	0.83

species, solvent motion driven by the injection of the excess electron into the solvent network.[48–52] For a binary complex such as I⁻U, only the first mechanism is operative.

Therefore, neutral iodine motion relative to the DB orbital of the uracil anion is likely responsible for the dynamics in Figure 3. Initially, the VDE of the DB anion is ∼75 meV, lower than our measured asymptotic value of 95 ± 5 meV, suggesting a repulsive interaction between the iodine atom and the DB anion. The VDE steadily increases (as shown in Fig 3(a)), reaching a maximum value of 115 meV by ∼700 fs, where there may be a favorable interaction between the iodine atom and the DB anion, before the VDE finally decreases to 95 ± 5 meV by approximately 20 ps (Figure 3(b)). By that time the iodine is either interacting less strongly with the DB orbital or has left the binary cluster.

These qualitative ideas are supported by recent theoretical work on I⁻U by Takayanagi and co-workers[25] and Takayanagi,[54] who performed CIS(D) calculations analyzing iodine movement relative to N1 after UV charge transfer to the uracil DB orbital from iodide. The potential energy curves show weak repulsion at small iodine-N1 distances and flatten at higher iodine-N1 distances, supporting the assignment of the initial VDE increase as a response to a repulsive interaction between the iodine and uracil DB anion.

At excitation energies of −110 meV and −40 meV, a clear rise time of ∼250 fs is seen for the DB state (Table I and Figure 4(a)), suggesting that a fully formed DB state is not created instantaneously by the pump pulse. Indeed, this rise time occurs on a time scale similar to that of the VDE shifting in Figure 3, during which the wavefunction of the excess electron is evolving as the iodine and nucleobase separate subsequent to photoexcitation.[25,47] Therefore, the intensity rise is likely a result of cross-section changes associated with this evolution. However, while the time-dependence of the VDE shifting is largely independent of excitation energy, the rise time τ_1 drops from 260 fs at -40 meV to 120 fs at 30 meV, and the ratio $|A_1|/(A_2 + A_3)$ drops from 0.46 to 0.28. This ratio represents the prominence of the signal with rise time τ_1 relative to the cross-correlated rise associated with the A_2 and A_3 terms. By 100 meV, the DB anion rises within the cross-correlation limit with no additional rising behavior ($A_1 = 0$). The dynamics responsible for this trend are discussed in Sec. IV C.

B. Early-time dynamics of the uracil valence bound anion

The 200–300 fs rise time of the VB anion at −110 meV to 100 meV compared to its cross-correlation limited rise at 550 meV implies that not only the dynamics but also the mechanism of electron attachment to uracil is highly dependent upon excitation energy. Our previous studies of I⁻U used excitation energies between 580 meV and 790 meV and the VB anion appeared with a cross-correlation limited rise time.[16] Experiments at intermediate excitation energies were attempted, but significant formation of neither the DB nor the VB anion was observed. It thus appears that there are two different mechanisms for VB anion formation, one at excitation energies near the VDE and another 550–790 meV above

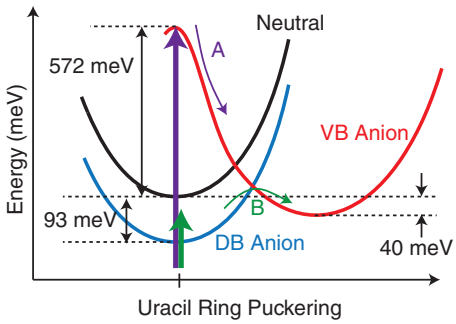

FIG. 6. Schematic potential energy curves for neutral uracil (black), the DB anion (blue), and the VB anion (red) plotted vs. uracil puckering angle. Tick mark on x-axis indicates planarity of the uracil ring. AEAs for the two anion states are shown,[18,29] along with the calculated vertical electron attachment energy (VAE), 572 meV, for the VB anion.[53] The vertical purple arrow represents a photon with excitation energy between 550 meV and 790 meV, where the VB anion is directly formed by mode A, while the vertical green arrow represents a photon with excitation energy between −110 meV and 100 meV and a possible mode B.

the VDE, while in between these regimes there is no efficient pathway for VB anion formation. These trends can be understood with reference to the energetic landscape of the uracil DB and VB anions. This landscape, based on the calculations by Bachorz *et al.*,[21] and experimental measurement of the uracil DB anion,[18] is depicted in Figure 6, which shows schematic potential energy curves for neutral uracil (black) as well as the anion DB and VB states (blue and red, respectively) as a function of the uracil puckering angle.

Absorption of a photon by the I⁻U complex is a vertical process. Barring any scattering resonances or bound states in either iodide or neutral uracil, the electron transfer process from iodide to uracil should also be approximately vertical, in the sense that the scattered electron will initially interact with the uracil in its original geometry, as shown in Figure 1, in which the neutral uracil is minimally perturbed by the iodide.[16] Therefore the uracil anion geometry directly after electron transfer is likely a planar structure very similar to the neutral geometry. The calculated vertical attachment energy (VAE) of the valence state in this planar geometry is 572 meV above the neutral.[53] As shown in Figure 6, at excitation energies in this range, indicated by the purple arrow, there is sufficient energy to form the VB anion directly in a planar geometry, and the VB anion is formed on a cross-correlation limited time via pathway A.

At excitation energies from −110 meV to 100 meV, shown by the green arrow in Figure 6, there is insufficient energy to form the VB anion directly. Table I shows that the rise time (τ_1) of the VB state is measurable across this interval, with the VB anion population increasing relative to the DB anion population as excitation energy increases, as indicated by the I/II ratio in Table I. The VB anion must be formed by an indirect pathway between −110 meV and 100 meV, and we propose in Sec. IV C that this pathway involves the DB anion, depicted as pathway B in Figure 6.

C. Dipole bound to valence bound anion transition

The geometry of uracil DB anion is very close to that of neutral uracil, and therefore the VAE to the DB state should

be approximately the negative of the VDE of the uracil DB anion, i.e. −93 meV,[18] as shown in Figure 6, making formation of the DB anion efficient at excitation energies near the VDE. At excitation energies from −110 to 100 meV we observe the DB state prominently at short delay times (<500 fs). The rise time of the VB state is either equal to or slower than that of the DB state. These results suggest that near the VDE, direct detachment to the DB anion occurs, and raise the question of whether the DB anion acts as a doorway to the VB anion. Evidence for such a mechanism is not as clear as it was for $I^-CH_3NO_2$ complexes, where we observed a decay of the nitromethane DB anion matching the rise time of the VB anion.[35] Complementary decay and rise times are not seen for I^-U, suggesting that if such a doorway mechanism occurs, there is incomplete conversion from the DB to the VB state.

The barrier between the DB and VB states has never been measured experimentally and calculated values vary with different levels of theory, between 36 and 178 meV.[22,23,25] Calculations using long range corrected DFT yield the lowest value, 36 meV and are expected to be the most accurate given the diffuse nature of the DB orbital.[25] Given the bandwidth of the excitation pulse in our experiment, 40 meV, combined with incomplete vibrational cooling of the I^-U anion, a DB to VB transition should be energetically feasible to varying extents from −110 meV to 100 meV. Indeed, the observed trend in the feature I/II ratio (Table I) is consistent with the notion that the DB to VB anion transition is facilitated as the excitation energy increases.

Recent calculations by the Takayanagi group[22,23] have investigated the nature of the charge transfer state from iodide to uracil. They find that the initial state is either a DB anion or a hybrid DB/σ^* anion, and that the transition to the π^* VB anion can easily occur with puckering of the uracil ring and out of plane movement of the C6 hydrogen by approximately 25°. The presence of iodine may also be relevant to the transition. Iodine, like xenon, is highly polarizable and may slightly alter the relative energies of the DB and VB anions, making a transition more energetically accessible before it leaves the binary cluster.

A DB to VB anion transition could also provide an explanation for why the rising behavior of the DB anion with time constant τ_1 becomes less prominent relative to the cross-correlated rise with increasing excitation energy. There are numerous processes in the I^-U complex that occur on similar timescales of 200–300 fs: the VDE shifting of the DB anion, the rise time of the DB anion at −110 meV and −40 meV, and the rise time of the VB anion. If the DB anion is indeed the doorway to the VB anion, the timescale of the DB anion decay to the VB anion is also 200–300 fs. At higher excitation energies, where there is comparatively more decay to the VB anion (Table I), the combination of the DB anion population decay to the VB anion and the DB anion intensity rise due to cross-section changes from iodine dynamics can effectively cancel each other out. This changes both the rise time of the DB anion signal as well as the intensity of that rise at those excitation energies, as observed at 30 meV and 100 meV. The addition of a new decay component to Eq. (2) with a similar lifetime to τ_1, representing the decay of the DB anion to the VB anion, effectively reduces the ratio $|A_1|/(A_2 + A_3)$ relative to lower excitation energies where the DB to VB anion decay is less important.

A dipole-bound to VB transition also offers a reasonable explanation for the rise time of the VB anion at excitation energies near the VDE. In contrast to nitromethane, where the VB anion state lies lower in energy than the DB anion, the VB anion for uracil is higher in energy than the DB anion, presumably explaining the incomplete conversion of the DB to the VB state. The decrease in the ratio of features I/II with increasing excitation energy is consistent with overcoming a barrier and energy gap for this transition. Overall, however, the evidence for the DB to VB anion transition in uracil is indirect rather than definitive.

D. Bi-exponential decay of the dipole bound and valence bound anions

We turn now to the longer-time decay dynamics of the DB and VB anions. Upon formation, both the DB and VB anions decay bi-exponentially. Bi-exponential decay is suggestive of parallel decay processes according to Scheme 1 (Sec. III), where the final state III is an autodetachment state of the uracil transient negative ions. Our previous papers on I^-U and I^-T defined state I as $I^{\cdots}U^-$ and state II as $I + U^-$, where k_1 and k_3 are differing rates of autodetachment prior and subsequent to iodine loss, and k_2 is the rate of iodine loss.[15,16] An analysis of the fractions in each decay pathway as well as the relative decay constants allows for the direct calculation of those rates, as detailed in Sec. III. The resulting calculated rate constants are listed in Table II. At all excitation energies, we find that $k_1 > k_2 > k_3$ for both the DB and VB anions. This ordering is consistent with autodetachment before and after iodine loss, because we expect that iodine loss reduces the internal energy of the remaining uracil anion, resulting in slower autodetachment. However, raising the excitation energy from 4.21 to 4.66 eV results in an increase in k_1 by nearly a factor of 20 for the VB state, and brings into question whether iodine loss is the only process that affects the autodetachment rate.

It is therefore of interest to consider other mechanisms for the bi-exponential decay. For example, if the uracil anion is initially formed with a non-statistical vibrational energy distribution, then k_1 can represent the autodetachment rate from this distribution, k_2 the rate of internal vibrational energy redistribution (IVR), and k_3 the autodetachment rate from a statistical vibrational energy distribution. This mechanism is similar to that proposed by Knee *et al.*[43] in the paper where Eq. (4) was derived, with the underlying assumption that the vibrational mode (or modes) in the initial distribution is strongly coupled to autodetachment.

This latter mechanism may well be operative in the VB anion at excitation energies 550 meV to 790 meV. When the VB anion is formed directly at those excitation energies, the initial VB anion geometry is planar and significantly perturbed from the equilibrium geometry of the VB anion.[29] Therefore the VB anion will be initially vibrationally excited specifically along the modes that transition between the planar and puckered geometries. State I would be a vibrationally

excited state with energy concentrated in the puckering modes and state II a state with vibrational energy fully distributed throughout all vibrational modes. Given that the potential energy curves for the VB and neutral state cross at an intermediate non-planar geometry (see Figure 6), it is reasonable to expect that the initially prepared vibrational distribution will be more strongly coupled to autodetachment compared to a statistical distribution with the same total energy, leading to $k_1 \gg k_3$, as is observed here at 4.66 eV. At lower excitation energies, where the VB state is not accessed directly, it is more difficult to envision a similar scenario and the iodine atom loss mechanism is more likely to dominate.

V. CONCLUSION

The dynamics of electron attachment to uracil are highly sensitive to excitation energy. At excitation energies −110 meV to 100 meV, both the DB and the VB anion of uracil are formed, while at 550 meV only the VB anion is observed. At −110 meV and −40 meV, the DB anion photoelectron signal has a 240–260 fs rise time, attributed to evolution of the wavefunction of the dipole-bound electron as the iodine moves relative to the DB anion. This rise time becomes less prominent, disappearing by 100 meV, where the DB anion rises on a cross-correlation limited time as decay of the DB anion to the VB anion possibly cancels the iodine-motion-related rising intensity.

The VB anion has a 200–300 fs rise time for excitation energies −110 meV to 100 meV, which is likely due to a DB to VB anion transition. At higher excitation energies, where there is sufficient photon energy to directly access the VB anion from the iodide-uracil anion initial state, the VB anion appears within the cross-correlation. Both states at all excitation energies subsequently undergo bi-exponential decay due to iodine loss or IVR, with IVR the more likely mechanism for the VB anion at 550 meV, where the VB anion can be formed directly.

These early-time electron attachment dynamics provide information about the necessary energies to directly form valence anions of uracil without the aid of dipole bound anion doorway states and draw into question whether the DB anion assists in electron capture at electron energies between 0.6 and 1 eV, as has been invoked in studies of dissociative electron attachment in uracil.[13] We also identify a possible timescale for the DB to VB anion transition in uracil, which will be of interest in future studies of the mechanisms of DNA and RNA damage by low-energy electrons.

ACKNOWLEDGMENTS

The work described in this paper was funded by the National Science Foundation (NSF) under Grant No. CHE-1011819. M.A.Y. gratefully acknowledges support from a NSF Graduate Research Fellowship. A.B.S. gratefully acknowledges support from The Villum Foundation.

[1]B. Boudaïffa, P. Cloutier, D. Hunting, M. A. Huels, and L. Sanche, Science **287**, 1658 (2000).
[2]E. Alizadeh and L. Sanche, Chem. Rev. **112**, 5578 (2012).
[3]J. Simons, Acc. Chem. Res. **39**, 772 (2006).
[4]J. Gu, Y. Xie, and H. F. Schaefer, J. Am. Chem. Soc. **128**, 1250 (2006).
[5]J. Gu, J. Leszczynski, and H. F. Schaefer, Chem. Rev. **112**, 5603 (2012).
[6]G. Hanel, B. Gstir, S. Denifl, P. Scheier, M. Probst, B. Farizon, M. Farizon, E. Illenberger, and T. D. Märk, Phys. Rev. Lett. **90**, 188104 (2003).
[7]A. Scheer, K. Aflatooni, G. Gallup, and P. Burrow, Phys. Rev. Lett. **92**, 068102 (2004).
[8]A. M. Scheer, C. Silvernail, J. A. Belot, K. Aflatooni, G. A. Gallup, and P. D. Burrow, Chem. Phys. Lett. **411**, 46 (2005).
[9]S. Ptasińska, S. Denifl, V. Grill, T. D. Märk, E. Illenberger, and P. Scheier, Phys. Rev. Lett. **95**, 093201 (2005).
[10]C. Winstead and V. McKoy, J. Chem. Phys. **125**, 174304 (2006).
[11]I. González-Ramírez, J. Segarra-Martí, L. Serrano-Andrés, M. Merchán, M. Rubio, and D. Roca-Sanjuán, J. Chem. Theory Comput. **8**, 2769 (2012).
[12]S. Denifl, S. Ptasińska, G. Hanel, B. Gstir, M. Probst, P. Scheier, and T. D. Märk, J. Chem. Phys. **120**, 6557 (2004).
[13]P. D. Burrow, G. A. Gallup, A. M. Scheer, S. Denifl, S. Ptasińska, T. D. Märk, and P. Scheier, J. Chem. Phys. **124**, 124310 (2006).
[14]G. A. Gallup and I. I. Fabrikant, Phys. Rev. A **83**, 012706 (2011).
[15]S. B. King, M. A. Yandell, and D. M. Neumark, Faraday Discuss. **163**, 59 (2013).
[16]M. A. Yandell, S. B. King, and D. M. Neumark, J. Am. Chem. Soc. **135**, 2128 (2013).
[17]N. A. Oyler and L. Adamowicz, J. Phys. Chem. **97**, 11122 (1993).
[18]J. Hendricks, S. Lyapustina, H. L. de Clercq, J. Snodgrass, and K. Bowen, J. Chem. Phys. **104**, 7788 (1996).
[19]C. Desfrançois, H. Abdoul-Carime, and J.-P. Schermann, Int. J. Mod. Phys. B **10**, 1339 (1996).
[20]O. H. Crawford, Mol. Phys. **20**, 585 (1971).
[21]R. A. Bachorz, W. Klopper, M. Gutowski, X. Li, and K. H. Bowen, J. Chem. Phys. **129**, 054309 (2008).
[22]T. Sommerfeld, J. Phys. Chem. A **108**, 9150 (2004).
[23]T. Takayanagi, T. Asakura, and H. Motegi, J. Phys. Chem. A **113**, 4795 (2009).
[24]H. Motegi and T. Takayanagi, J. Mol. Struct (THEOCHEM) **907**, 85 (2009).
[25]Y. Yokoi, K. Kano, Y. Minoshima, and T. Takayanagi, J. Comput. Theor. Chem. **1046**, 99 (2014).
[26]J. Hendricks, S. Lyapustina, H. L. de Clercq, and K. Bowen, J. Chem. Phys. **108**, 8 (1998).
[27]R. N. Compton, H. S. Carman, C. Desfrançois, H. Abdoul-Carime, J. P. Schermann, J. H. Hendricks, S. A. Lyapustina, and K. H. Bowen, J. Chem. Phys. **105**, 3472 (1996).
[28]J. Schiedt, R. Weinkauf, D. M. Neumark, and E. W. Schlag, Chem. Phys. **239**, 511 (1998).
[29]R. A. Bachorz, W. Klopper, and M. Gutowski, J. Chem. Phys. **126**, 085101 (2007).
[30]M. D. Sevilla, B. Besler, and A.-O. Colson, J. Phys. Chem. **99**, 1060 (1995).
[31]C. Desfrançois, V. Periquet, Y. Bouteiller, and J. Schermann, J. Phys. Chem. A **102**, 1274 (1998).
[32]P. Dedíková, L. Demovič, M. Pitoňák, P. Neogrády, and M. Urban, Chem. Phys. Lett. **481**, 107 (2009).
[33]D. Roca-Sanjuán, M. Merchán, L. Serrano-Andrés, and M. Rubio, J. Chem. Phys. **129**, 095104 (2008).
[34]A. Stolow, A. E. Bragg, and D. M. Neumark, Chem. Rev. **104**, 1719 (2004).
[35]M. A. Yandell, S. B. King, and D. M. Neumark, J. Chem. Phys. **140**, 184317 (2014).
[36]F. Edard, and M. Tronc, J. Phys. B: At. Mol. Phys. **20**, L265 (1987).
[37]R. Hashemi and E. Illenberger, J. Phys. Chem. **95**, 6402 (1991).
[38]A. V. Davis, R. Wester, A. E. Bragg, and D. M. Neumark, J. Chem. Phys. **118**, 999 (2003).
[39]A. E. Bragg, J. R. R. Verlet, A. Kammrath, O. Cheshnovsky, and D. M. Neumark, J. Am. Chem. Soc. **127**, 15283 (2005).
[40]A. T. J. B. Eppink, and D. H. Parker, Rev. Sci. Instrum. **68**, 3477 (1997).
[41]V. Dribinski, A. Ossadtchi, V. Mandelshtam, and H. Reisler, Rev. Sci. Instrum. **73**, 2634 (2002).
[42]M. A. Yandell, Ph.D. dissertation, University of California, Berkeley, 2014.
[43]J. L. Knee, L. R. Khundkar, and A. H. Zewail, J. Chem. Phys. **87**, 115 (1987).
[44]A. Kammrath, J. R. R. Verlet, E. Arthur, G. B. Griffin, and D. M. Neumark, J. Phys. Chem. A **109**, 11475 (2005).
[45]O. T. Ehrler, G. B. Griffin, R. M. Young, and D. M. Neumark, J. Phys. Chem. B **113**, 4031 (2009).

[46]R. M. Young, M. A. Yandell, and D. M. Neumark, J. Chem. Phys. **134**, 124311 (2011).
[47]C. C. Mak, Q. K. Timerghazin, and G. H. Peslherbe, J. Phys. Chem. A **117**, 7595 (2013).
[48]Q. K. Timerghazin and G. H. Peslherbe, Chem. Phys. Lett. **354**, 31 (2002).
[49]T. Takayanagi and K. Takahashi, Chem. Phys. Lett. **431**, 28 (2006).
[50]M. Kołaski, H. M. Lee, C. Pak, and K. S. Kim, J. Am. Chem. Soc. **130**, 103 (2007).
[51]W.-S. Sheu, and M.-F. Chiou, J. Phys. Chem. A **117**, 13946 (2013).
[52]C. C. Mak and G. H. Peslherbe, J. Phys. Chem. A **118**, 4494 (2014).
[53]R. A. Bachorz, J. Rak, and M. Gutowski, Phys. Chem. Chem. Phys. **7**, 2116 (2005).
[54]T. Takayanagi (private communication, 2014).